Photochemical Z→E Isomerization of a Hemithioindigo/Hemistilbene ω-Amino Acid

ARTICLE · JANUARY 2007

READS
19

8 AUTHORS, INCLUDING:

Tobias Schrader
Forschungszentrum Jülich
64 PUBLICATIONS **1,041** CITATIONS
SEE PROFILE

Karola Rück-Braun
Technische Universität Berlin
68 PUBLICATIONS **824** CITATIONS
SEE PROFILE

DOI: 10.1002/cphc.200700223

Photochemical $Z \rightarrow E$ Isomerization of a Hemithioindigo/Hemistilbene ω-Amino Acid

Thorben Cordes,[a, b] Björn Heinz,[a, b] Nadja Regner,[a, b] Christian Hoppmann,[c] Tobias E. Schrader,[a, b] Wolfram Summerer,[a, b] Karola Rück-Braun,[c] and Wolfgang Zinth*[a, b]

The molecule HTI, which combines hemithioindigo and hemistilbene molecular parts, allows reversible switching between two isomeric states. Photochromic behaviour of the HTI molecule is observed by irradiation with UV/Vis light. The photochemical reaction, a Z/E isomerization around the central double bond connecting the two molecular parts, is investigated by transient absorption and emission spectroscopy. For a special HTI molecule, namely, an ω-amino acid, the Z→E isomerization process occurs on a timescale of 30 ps. In the course of the reaction fast processes on the 1–10 ps timescale are observed which point to motions of the molecule on the potential-energy surface of the excited state. The combination of transient absorption experiments in the visible spectral range with time-resolved fluorescence and infrared measurements reveal a photochemical pathway with three intermediate states. Together with a theoretical modelling procedure the experiments point to a sequential reaction scheme and give indications of the nature of the involved intermediates.

1. Introduction

Photoinduced isomerizations are highly important prototypical reactions for chemistry and biology.[1–3] Small molecules containing conjugated double bonds (e.g. stilbene, hexatriene) are used as model systems to investigate ultrafast photochemistry and to obtain a detailed understanding of the underlying molecular processes. Photochromic compounds can also be used as optical switches for data storage,[4] as ultrafast structural switches to induce molecular transitions, or as driving units for nanomachinery.[5–8] In addition, peptides containing light-triggered groups have been used to study the fastest processes in peptide folding.[5–7,9] Another important potential application of photochromic compounds is photomediated in vivo on/off switching of the activity of therapeutic compounds.[10,11]

Different types of basic structures are used as photochromic centres, for example, stilbene and azobenzene.[5,6] To give an insight into the mechanisms of *Z*/*E* isomerization, we review the literature data on the photoreaction of stilbene, because of the structural conformity with the investigated HTI molecule. Various experimental and theoretical studies addressing this issue can be found.[2,3,12] Orlandi and Siebrand[13] suggested a model with two excited-state potential surfaces and a simplified reaction coordinate, that is, the rotation around the central double bond with a dihedral angle ϕ. This model was extended by Hohleichner and Dick.[14] The electronic ground state can be described by a potential curve showing two minima at $\phi = 0$, 180° and a maximum for $\phi = 90°$. The one-electron excited state S_1(B) shows two minima at $\phi = 0$, 180° and a maximum at $\phi = 90°$. This state crosses the doubly excited state S_2(A), which has two maxima at $\phi = 0$, 180° and a minimum at $\phi = 90°$. Mixing of the two states results in formation of a barrier on the excited-state potential surface. After excitation to the S_1(B) state, the molecule starts to twist around its double bond. Access to the biradicaloid minimum at $\phi = 90°$ is hindered by the barrier. The existence of a barrier on the exited-state potential surface has been shown by means of temperature-dependent quantum-yield measurements by Saltiel et al.[15] Once the molecule has overcome this barrier, it reaches a structure with strong charge-transfer character (P*)[16,17] from where internal conversion to the ground state takes place. This transition can also be described via a conical intersection (CoI) by using a more complex reaction coordinate.[18,19] The timescale of the complete photoreaction is determined by the barrier height and hence the accessibility of P*/CoI. The barrier height for stilbene varies with substitution and the specific surroundings (solvent, temperature). The esti-

[a] *T. Cordes, B. Heinz, N. Regner, T. E. Schrader, W. Summerer, Prof. Dr. W. Zinth*
Lehrstuhl für BioMolekulare Optik
Department für Physik, Ludwig-Maximilians-Universität
Oettingenstr. 67, 80538 München (Germany)
Fax: (+49) 89-2180-9202
E-mail: wolfgang.zinth@physik.uni-muenchen.de

[b] *T. Cordes, B. Heinz, N. Regner, T. E. Schrader, W. Summerer, Prof. Dr. W. Zinth*
Munich Center for Integrated Protein Science CIPS^M(Germany)

[c] *C. Hoppmann, Prof. Dr. K. Rück-Braun*
Technische Universität Berlin, Institut für Chemie
Straße des 17. Juni 135, 10623 Berlin (Germany)

mated value for an isolated molecule in the gas phase is 3.4 kcal mol^{-1}.[20]

In a recent paper we investigated a special type of HTI molecule.[7] We demonstrated that the HTI structure is well suited for biological applications since it can be built into cyclic or linear peptide structures without losing its photochromic capabilities. The investigated HTI ω-amino chromopeptides show ultrafast isomerization reactions in the 30–60 ps time range. Fast absorption transients point to motions of the molecule on the excited-state potential surface within 1–10 ps. The rate of isomerization was determined by time-resolved absorption (TA) measurements.[7] A more detailed description of the excited-state dynamics of HTI requires additional experimental information. These data would lead to an improved understanding of the underlying reaction mechanisms and would facilitate the design of photochromic compounds optimized for a specific switching problem.

Time-resolved absorption experiments monitor electronic transitions in the visible spectral range. Here the absorption changes result from population transfers of different electronic states induced by the excitation process. These processes comprise reduced absorption from the original ground-state molecules (ground-state bleaching, GSB), stimulated emission (SE), and excited-state absorption (ESA) due to the population of electronically excited states. In addition, intermediates and products formed in the course of the reaction appear, as well as transient absorption changes within one electronic state due to solvation and vibrational relaxation. In visible TA experiments, all different processes may contribute to the signal. Since the various visible absorption bands are broad and featureless, it is difficult to acquire a conclusive picture of the reaction from TA data alone. To get additional information other techniques are required: A clear assignment of an intermediate to an electronically excited state can be obtained by time-resolved observation of its emission in transient fluorescence (TF) experiments. Detailed information on the presence of specific reaction products can be derived from time-resolved vibrational techniques, such as transient IR (TIR) or Raman spectroscopy.

Here we combine the known data from visible TA spectroscopy on the $Z \rightarrow E$ isomerization of the HTI ω-amino acid with results from time-resolved fluorescence and IR spectroscopy. We demonstrate that the reaction in the excited electronic state involves the transient population of three intermediate states. Modelling the difference absorption and emission spectra by a system of rate equations provides details of the reaction. The spectra of the different intermediates give clear insight into the relevant molecular processes and allow the isomerization of HTI to be related to those of stilbene and other photochromic compounds.[2,3,15–19]

Experimental Section

Materials and Stationary Spectroscopy: The synthesis of the hemithioindigo-based ω-amino acid (Scheme 1) has been described elsewhere.[21,22] For experiments in the visible range (transient absorption/transient fluorescence) the compound was dissolved in

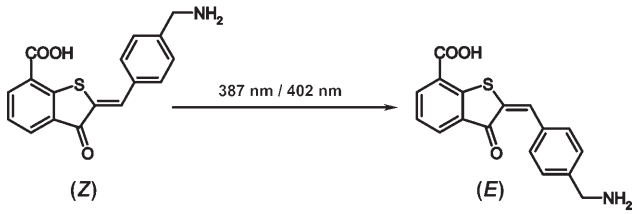

Scheme 1. Structures of the *Z* and *E*-isomers of the of HTI ω-amino acid photoswitch.

methanol (Merck, purity 99%). For IR experiments deuterated methanol (CD_3OD, Merck, purity 99.8%, degree of deuteration 99%) was used as solvent. Illumination of the sample with light at short wavelengths (peaks at 400/430 nm, mercury–xenon lamp, Hamamatsu, filtered with 3 mm optical filter GG385, Schott) forms a photostationary state (PSS400) containing approximately 85% *E*-isomer. In the dark the thermally unstable *E*-isomer reverts to the *Z*-form on a timescale of several hours.[21,22] Fast regeneration of the *Z*-isomer can be achieved by illumination at long wavelengths: A photostationary state containing more than 95% of the *Z*-isomer (PSS495) can be generated by using the output of a cold light source (KLC2500, Schott, filtered by a 3 mm long-pass filter GG495, Schott). During the femtosecond experiments the composition of the sample solution (*Z/E* ratio) was maintained in PSS495 by the use of the described exposure set-up. Flow cells and a peristaltic pump were used to exchange the sample solution between consecutive femtosecond pump pulses.

A spectrophotometer (Perkin-Elmer, Lambda 19) was employed to measure the continuous-wave (cw) UV/Vis absorption spectra. Fluorescence spectra were recorded on a standard fluorimeter (Specs, Fluorolog 1680, 0.22 m Double Spectrometer). The sample solutions were stirred and excited with monochromatic light at 402 nm. Steady-state IR spectra were recorded on an FTIR spectrometer (Bruker, IFS-66). Infrared difference spectra were obtained by exposure of the sample to short-wavelength light at 400/430 nm within the spectrometer housing. For this purpose the output of the mercury–xenon lamp (Hamamatsu) was filtered by a 3 mm optical filter GG385 (Schott) and directed onto the sample by a fiber-optic light guide.

Time-Resolved Spectroscopy: Time-resolved IR/Vis spectra were recorded in pump–probe set-ups based on a home-built Ti:sapphire laser/amplifier system (pulse duration 90 fs, centre wavelength 804 nm, pulse energy 1 mJ, repetition rate 1 kHz). The pump pulses (402 nm) were obtained by second-harmonic generation. The resulting absorption changes in the visible spectral range were recorded by a femtosecond white-light continuum used as probe pulse, combined with multichannel detection (350–650 nm).[23,24] Further details of the setup of the TA experiments can be found in refs. [5,7,23,24].

The generation of mid-IR probe pulses has been described in details elsewhere. The pump-induced absorption changes of the sample were recorded at a polarization of 45° between pump and probe. Parallel (ΔA_{pl}) and perpendicular (ΔA_{pp}) signals were simultaneously recorded with two spectrometers combined with 32-element mercury–cadmium–telluride (MCT) arrays. The two signals were transformed into one signal that is equivalent to magic-angle polarization according to $\Delta A_m = 1/3\,\Delta A_{pl} + 2/3\,\Delta A_{pp}$. A more detailed description of the infrared set-up can be found in ref. [25].

The transient fluorescence experiment is based on recording the fluorescence emission by an optical Kerr gate driven by femtosec-

ond NIR pulses (1100 nm). Excitation pulses were generated from the output of a femtosecond laser/amplifier system (Clark CPA 2001, 775 nm, 1 kHz). The output was frequency-doubled (387 nm) and focussed onto the sample cell (path length 1 mm). The resulting emission was collected by reflective optics and imaged onto a Kerr medium (fused silica plate) placed between two wire-grid polarizers. Gate pulses were generated by use of a two-stage optical parametric amplifier (OPA). Fluorescence light passing the Kerr gate was dispersed by a spectrometer (Acton Research, Spectra Pro 300i) and detected by a liquid-nitrogen-cooled CCD camera (Princeton Instruments, Spec-10:400B). The set-up showed a temporal resolution (full width of the instrumental response function) of approximately 150 fs. All spectra were corrected for the spectral sensitivity of the detection system, a λ^2 dependence of the gating procedure, and for group velocity dispersion induced by the set-up. Detailed information can be found in refs. [26, 27].

Modelling of the Data: To qualitatively interpret the recorded IR spectra of the *Z* and *E*-isomers, DFT calculations were performed on the B3LYP/6-31G** level as implemented in the Gaussian 98 programme package[28]. Both structures (*Z* and *E*-isomers) were geometry-optimized, and IR spectra were calculated for each isomer at the same level of theory.

A mathematical analysis of the transient absorption/fluorescence signals was performed according to the literature.[29,30] The analysis is based on the hypothesis that all investigated intermediates (number *n*) have well-defined spectroscopic properties, which depend on the population N_i, the absorption cross-section $\sigma_{i,\lambda}$, and emission cross-section $\rho_{i,\lambda}$ of the respective intermediate I_i at a specific observation wavelength λ. The optical excitation of the stable and non-fluorescing ground state I_0 results in a population change ΔN of intermediate I_1 at time zero. Subsequent population changes of a certain state I_i are determined by a system of rate equations [Eq. (1)].

$$\frac{dN_i(t)}{dt} = \sum_{j=0}^{n} K_{ij} N_j(t) \quad \text{for } i = 0...n \tag{1}$$

The individual rate constants K_{ij} for $i \neq j$ describe the population transfer from one state I_j to the other I_i. If the eigenvalues k_i of the rate matrix are not degenerate the population density $N_i(t)$ of a state I_i is a linear combination of $n+1$ exponentials [Eq. (2)].

$$N_i(t) = \sum_{j=0}^{n} N_{ij} e^{-k_j t} - \Delta N \delta_{i,0} \quad \text{for } t > 0 \tag{2}$$

When the total population of all states considered is constant during the transition of I_0 to I_n (i.e., there is no loss due to chemical reactions), one eigenvalue vanishes and *n* finite time constants are obtained. A sample with length *z* shows the following time dependence of the absorption $A_\lambda(t)$ and the fluorescence $F_\lambda(t)$ [Eqs. (3) and (4)].

$$\Delta A_\lambda(t) = \frac{z}{\ln(10)} \sum_{j=0}^{n} \sigma_{i,\lambda} N_i(t) \propto \sum_{j=0}^{n} a_{i,\lambda} e^{-k_j t} \quad \text{for } t > 0 \tag{3}$$

$$F_\lambda(t) \propto \sum_{j=1}^{n} \rho_{i,\lambda} N_i(t) \propto \sum_{j=1}^{n} f_{i,\lambda} e^{-k_j t} \quad \text{for } t > 0 \tag{4}$$

Within this description, emission and absorption have a multi-exponential time dependence (time constants $\tau_i = 1/k_i$) with the respective amplitude spectra $a_{i,\lambda}$ and $f_{i,\lambda}$. These amplitude spectra are often called decay-associated spectra (DAS) and should not be confused with the cross-section spectra ($\sigma_{i,\lambda}$, $\rho_{i,\lambda}$) or the transient spectra ($\Delta A_\lambda(t)$, $F_\lambda(t)$) observed at certain times *t*. The parameters N_{ij} [Eq. (2)] which determine the spectra are obtained by using the eigenvectors of the rate matrix for each eigenvalue and the specific starting condition (the population change of the initial state N_1 induced by the excitation). The presented procedure allows the time-dependent populations of the involved states to be calculated provided that the rate matrix is known. However, the rate matrix of an arbitrary molecular system cannot be obtained from a standard optical experiment. In order to tackle a typical spectroscopic problem, one measures the time dependence of absorption or emission spectra, models the data using a multi-exponential fit and gets *m* time constants and *m* amplitude spectra. Without additional knowledge on the reacting system, it is impossible to determine the complete $(m+1)\times(m+1)$ rate matrix from this information alone. In this situation the inversion of the problem, that is, determination of the individual reaction rates and spectra of the intermediates, is not possible. Only additional knowledge on the reacting system would help to determine the rate matrix and to invert the problem. This additional information may come from different experiments (e.g., via excitation to different states, modified samples) or from a theoretical treatment of the underlying reaction. Here we investigate different prototypical reaction models and show that most models lead to unrealistic spectral properties of the intermediates. These findings condense the multidimensional problem to a simple reaction model.

2. Results

2.1. Stationary Characterization: Absorption and Emission

The molecular structures of the two HTI isomers are shown in Scheme 1. The combination of hemistilbene and a hemithioindigo molecular parts to form the complete HTI molecule results in a strong absorption band (*Z*-form: $\lambda_{max} = 430$ nm, Figure 1a) in the blue part of the spectrum. Illumination of the *Z*-isomer in this region leads to a photostationary state (PSS400), which contains 85% of the molecules in the *E*-form. The *E*-isomer shows reduced oscillator strength and red-shifted absorption (peak at 450 nm) compared to the *Z*-isomer. The absorbance changes resulting from the $Z \rightarrow E$ switching process are shown in the lower panel of Figure 1a. They are dominated by strong bleaching at 430 nm and an increase in absorption at 460 nm. The cw fluorescence of the *Z*-isomer is shown as an inset. It displays a maximum around 500 nm. The isomerization quantum yield for the formation of the *E*-isomer in methanol at room temperature Φ_{PC} is 11% (illumination at 414 nm).[7]

The stationary IR spectrum of HTI and the absorption difference in the IR induced by isomerization are shown in Figure 1b. The absorption spectrum of the *Z*-form (solid curve, Figure 1b, upper part) is stronger than that of the *E*-form (PSS400, broken curve). The *Z*-form shows several distinct bands between 1550 and 1610 cm^{-1}, a spectral range characteristic for aromatic/olefinic carbon–carbon double bonds. These bands point to a strongly conjugated electron system, as expected for the planar *Z*-isomer. Other characteristic features in the 1650–1720 cm^{-1} region are related to the carboxyl and aromatic keto groups. Here the narrow band at 1690 cm^{-1} can be assigned to the aromatic keto group. The underlying broader band is due to the carboxyl group (maximum around

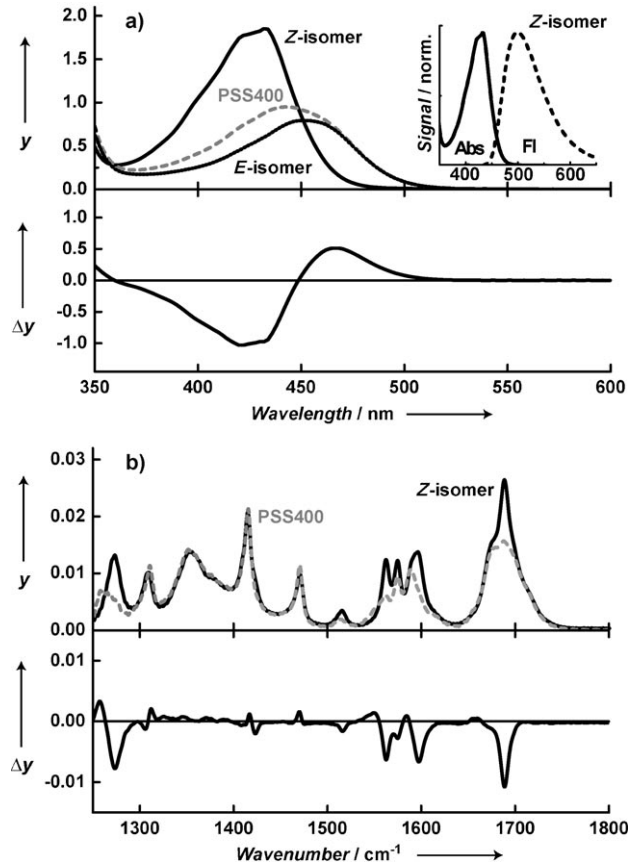

Figure 1. a) UV/Vis: The upper part shows the absorption spectra of the *Z*-isomer (black), PSS400 (broken, ca. 85% *E*-isomer) and the calculated spectrum of the *E*-isomer (black). Inset: Fluorescence (Fl) and absorption (Abs) spectra of the *Z*-isomer. The lower panel of a) shows the difference spectra for the switching process $Z \rightarrow E$. b) IR: The upper panel shows the IR spectra of the *Z*-isomer (black) and PSS400 (broken, ca. 85% *E*-isomer). The lower panel shows the difference spectra for the switching process $Z \rightarrow E$. *y*: Absorbance/OD.

1680 cm^{-1}). The unexpected high frequency of the keto group compared to the carboxyl group is due to the heterocyclic structure of the five-membered ring containing the keto group. Normal-mode analysis for both CO groups (performed with Gaussian 98 at the B3LYP/6-31G** level) qualitatively confirmed the assignment of the two CO oscillators.

Isomerization of the HTI molecule leads to strong changes in the IR spectrum (see Figure 1b). The pronounced keto band of the *Z*-form and the bands related to the aromatic/olefinic carbon–carbon double bonds lose intensity during the $Z \rightarrow E$ reaction. This can be explained by changes in the molecular geometry and the surroundings of the keto group. Due to steric hindrance between an aromatic hydrogen atom and the keto oxygen atom, the structure of the *E*-isomer deviates from planarity. This not only influences the IR spectrum but also leads to a reduction of oscillator strength in the visible spectrum, as shown in the upper panel of Figure 1a. The pronounced changes in the IR spectrum between 1550 and 1720 cm^{-1} with several marker bands for the $Z \rightarrow E$ reaction allow the isomerization to be followed by transient IR spectroscopy with high temporal resolution (see below).

2.2. Time-Resolved Measurements: Transient Absorption (Vis) and Fluorescence Experiments

The $Z \rightarrow E$ photoisomerization initiated by near-UV light was investigated by means of transient absorption and transient fluorescence spectroscopy (Figure 2). The upper graphs (Figure 2a, c) show transient spectra $\Delta A_\lambda(t)$ and $F_\lambda(t)$ taken at certain delay times t_D between pump and probe/gate pulse. For closer inspection of the involved dynamics, the transient data sets were fitted by multi-exponential model functions with wavelength-independent time constants. The amplitude spectra $a_{i,\lambda}$ and $f_{i,\lambda}$ related to the different time constants τ_i are presented in Figures 2b and d. Errors in the time constants corresponding to the DAS are 20% for all experiments.

In the case of transient absorption we observe a broad excited-state absorption (ESA) throughout the whole investigated spectral range (360–670 nm) at early delay times ($t_D = 0.5$ ps, Figure 2a). The ESA signal is superimposed by ground-state bleaching (GSB) centred around 430 nm and stimulated emission at 460 nm, which is blue-shifted compared to the cw fluorescence. In the transient spectrum taken at a time delay of 5 ps, a growth in absorption at 460 nm combined with a reduction of the absorption at 550 nm is observed. At delay times of 20–50 ps the absorption signal decays towards a weak, long-lasting absorption difference. This difference (e.g. at 150 ps) is due to formation of the *E*-isomer and resembles the $Z \rightarrow E$ cw difference spectrum shown in Figure 1a. Modelling of the experimental data shows that the fast processes which occur within the first picoseconds show some deviations from exponential fit functions. In addition singular-value decomposition does not yield information on the number of involved time constants. The transients can thus be approximated by either one or two exponential fit functions in the time regime of 1–10 ps. In ref. [7] two exponentials were used, but the use of only one component with a time constant of 4.5 ps (Figure 2b) also results in an adequate description of the data. We therefore use only the time constant of 4.5 ps herein. During this time the blue-shifted emission is reduced while the superimposed signal decreases for longer wavelengths. No significant loss of oscillator strength can be observed for this process. The subsequent decay of the complete signal is fitted with 33 ps (Figure 2b) and marks the end of the photoreaction.

Time-resolved fluorescence measurements (see the transient emission spectra taken at specific delay times in Figure 2c) exhibit the following qualitative features. At $t_D = 0.2$ ps (Figure 2c) we observe a fluorescence spectrum peaking at 475 nm. This early emission spectrum is strongly blue-shifted compared to the stationary fluorescence spectrum (Figure 1), where the maximum is found around 500 nm. Within hundreds of femtoseconds the emission spectrum slightly shifts to longer wavelengths. Subsequently, the fluorescence intensity decays bi-exponentially with a distinct wavelength dependence. At short wavelengths (< 470 nm) the emission decreases on the 5 ps timescale, whereas the emission at longer wavelengths vanishes within tens of picoseconds. A multi-exponential fit with three time constants of 200 fs, 4.7, and 27 ps repro-

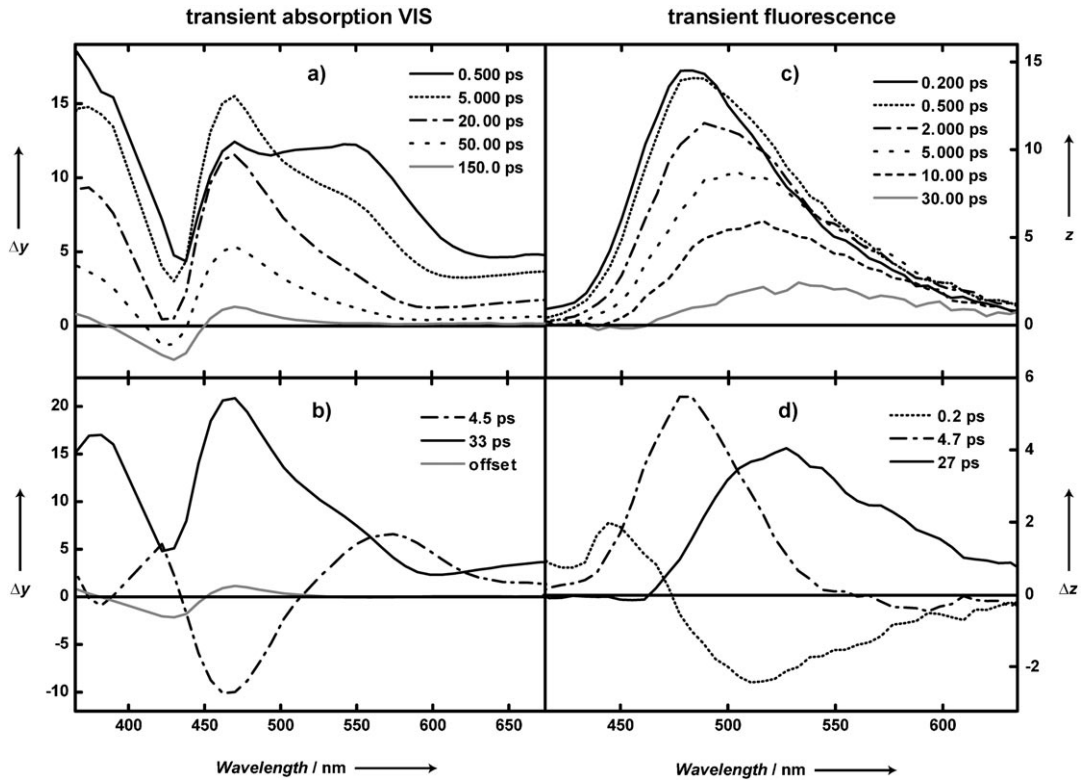

Figure 2. Results from transient absorption (a,b) and fluorescence (c,d) experiments. The Figure shows transient spectra $\Delta A_\lambda(t)$, $F_\lambda(t)$ at certain delay times (upper panel) and amplitude spectra $a_{i,\lambda}$ and $f_{i,\lambda}$ (lower panel) derived from a global fitting routine for the switching process of the HTI molecule. *y*: Absorbance/mOD; *z*: Fluorescence intensity/a.u..

duces the experimental emission data. The fitting amplitudes related to the three time constants are plotted in Figure 2 d.

2.3. Transient Absorption in the IR Region

The transient absorption changes recorded in the range of the CO stretching modes are shown in Figure 3. Early transient spectra ($t_D < 0.5$ ps) show optical nonlinearities connected with the excitation process[31] and initial reaction dynamics. After 1 ps one finds a pronounced decrease in absorption of the original CO stretching band around 1680 cm^{-1}. In addition, there is a broad absorption increase at other frequencies. Such behaviour is indicative of an excited electronic state. Only minor changes in absorption occur in the next 10 ps. However, a strong change in the absorption is seen in the 30 ps time domain, where the increased absorption and most of the bleaching disappear. At delay times longer than 1 ns we find a narrow absorption decrease at 1688 cm^{-1}. The position of this band and its amplitude match the formation of the *E*-isomer with a quantum yield of 11 %.[7] A more detailed picture is obtained by a multi-exponential fit of the data for delay times exceeding 1 ps (amplitude spectra shown in Figure 3 b). Again, we find time constants in the range of a few picoseconds (2.4 and 34 ps). In addition, there is a slower kinetic component associated with a time constant of 600 ps. Due to its broad spectral shape and its spectral position within the range of the carboxyl modes, this component can tentatively be assigned to reorientation of the carboxyl group and its surroundings, which cannot be observed in the visible spectral range. The strong amplitude of the 34 ps component modelling the decay of both the bleaching of the CO bands and the broad induced absorption, clearly shows that the transition to the electronic ground state (*Z* or *E*) of the HTI must be associated with the 30 ps process. This strongly supports the findings from the transient fluorescence experiment and the interpretation given in ref. [7]. The amplitude spectrum of the 2.4 ps kinetic component is of special interest. This spectrum features no recovery of the bleaching of the CO band, but some changes in the broad absorption increase are found. One can interpret this behaviour in terms of rearrangement and relaxation of the HTI molecule in the excited electronic state. There is no indication for internal conversion to the ground state with the time constant of 2.4 ps.

The experimental results from the transient absorption experiments in the Vis and IR regions and from transient fluorescence can be summarized as follows: After optical excitation three processes with time constants of 200, 4, and 30 ps are observed, which lead to the absorption changes found in the femtosecond data sets. The spectral amplitudes related to the different dynamics indicate that pronounced excited-state reactions occur with a strong decrease of the blue part of the emission spectrum prior to internal conversion to the electronic ground state with a time constant of 30 ps.

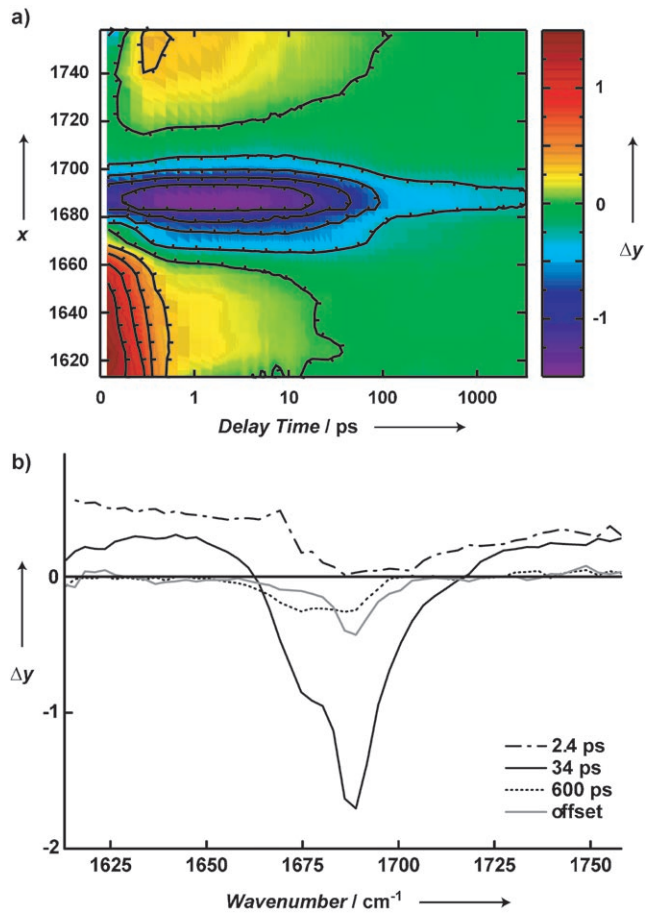

Figure 3. a) Transient IR data shown as two-dimensional spectrum of the investigated spectral range versus delay time. Note the linear timescale from 0 to 1 ps and the logarithmic timescale thereafter. b) Kinetic analysis applied to the data with resulting decay-associated spectra. *x*: Wavenumber/cm^{-1}; *y*: Absorbance/mOD.

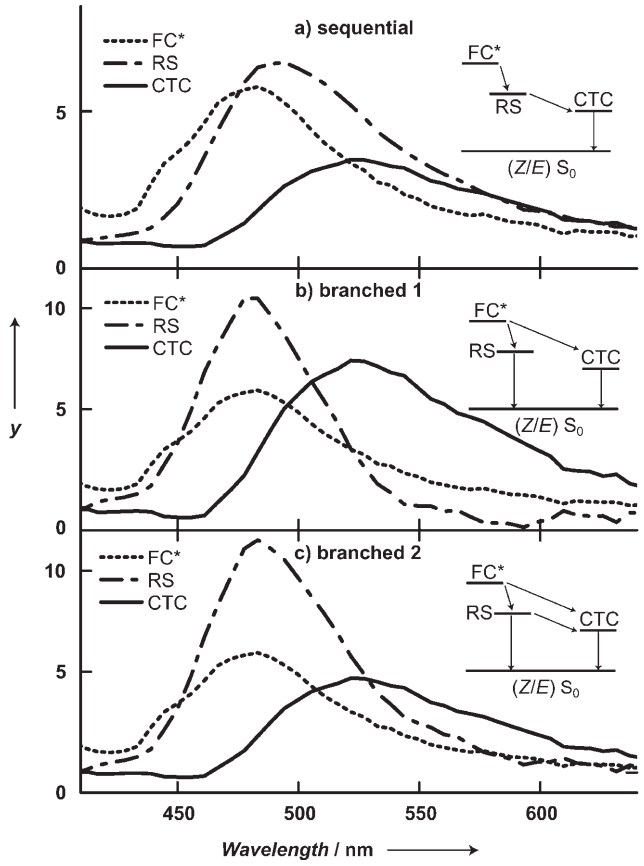

Figure 4. Calculated fluorescence spectra $\rho_{i,\lambda}$ for different state models. a) Sequential case, b) pure branched model and c) mixed version. Schematic state models are shown as insets. *y*: Fluorescence intensity/a.u..

3. Discussion: Modelling the Data

The experimental observations with three picosecond time constants suggest that a reaction model must be considered in which three intermediates (I_1, I_2, I_3) exist in addition to the ground-state isomers *Z* and *E*. Without any further restrictions on the rate-equation model we would have to consider $n=4$ reaction rates to and from every state. Fortunately, the structure of the molecular reaction scheme and the qualitative analysis of the experimental results reduce the number of potential reaction paths. The large energy gap between the electronic ground states *Z* and *E* prevents reactions forming the electronically excited intermediates I_1 to I_3 without optical excitation. The simplest reaction model is a pure sequential model, in which the reaction starts at I_1 and continues via I_2 to I_3, whereby internal conversion to the ground state forms the *Z* or *E*-isomer. Other reaction models would imply early branching of the originally populated intermediate I_1 to I_2 and I_3 and additional internal conversion processes of I_1 and I_2. In the following discussion of the transient data, we focus on the simple sequential model before we show the consequences of branching for the spectral properties of the intermediates. Using the procedure described in the Experimental Section makes it possible to calculate the transient spectra of the intermediate states. Figure 4 gives an overview of the transient fluorescence spectra for the three involved states I_1, I_2, and I_3 for different reaction models. The figure shows the situation for the sequential (Figure 4a) and two branched models (Figures 4b and 4c).

3.1. Sequential Reaction Model

Excitation of HTI by UV/Vis light populates the Franck–Condon region (FC*, I_1) of the *Z*-isomer in a vertical transition without changing the nuclear configuration. The fluorescence spectrum of this state is shown in Figure 4a (broken line). It is well known that optical excitation generates the excited electronic state with a huge amount of vibrational excess energy. In addition, displacement of the electron density can occur which then leads to (partial) inversion of single- and double-bond characters. Both processes induce ultrafast reactions that rapidly follow the excitation process. The changed charge distribution forces fast rearrangement of the solvent cage (solvation), while the excess of vibrational energy leads to fast initial configurational changes and intramolecular vibrational energy relaxation (IVR). The molecular state populated in this reaction can be described as a relaxed state (RS, I_2). These molecular

processes are connected with the 200 fs time constant. The corresponding amplitude spectrum shows that the fluorescence emission is slightly red-shifted and that the high-frequency stimulated emission in the visible transient absorption experiments disappears. The emission spectrum of the RS state is shown as the dash-dotted curve in Figure 4a. The spectral shift connected with the FC*→RS transition shows no significant change in oscillator strength. The secondary process with a time constant of about 4 ps causes the disappearance of the blue part of the emission spectrum and a related strong decrease of the oscillator strength (solid curve in Figure 4a). This red shift can be taken as an indication of structural distortions along the reaction coordinate connected with a charge-transfer process.[32] As a consequence, the molecular state reached in the this process may have some charge-transfer character (CTC state, I_3). Quantum chemical calculations for related model compounds have shown that the region of the excited-state potential surface where the transition to the ground state takes place has considerable charge-transfer character.[2,3,12,15–17] Here the transition to the ground-state potential-energy surface may occur via P* with a small energy gap to the ground state combined with a conical intersection (CoI).[2,3,12,15–19] In both cases the reaction rate to the ground-state photoproduct is limited by access of a molecule in the CTC state to the transition region. This reaction step can be related to the process with a time constant of about 30 ps. From a qualitative point of view the sequential model seems to be an adequate description for the processes observed after excitation of HTI at 400 nm.

3.2. Reaction Models with Branching

In the reaction model shown in Figure 4b we assumed that branching occurs with 200 fs from the Franck–Condon state FC* (I_1). The two states RS and CTC are formed in parallel. Both states decay directly to the ground state (*Z* or *E*) with time constants of about 4 ps (RS) and about 30 ps (CTC). In calculating the spectra of Figure 4b, we assumed that both states are formed with the same efficiency. The spectrum of the RS state, which decays faster (dash-dotted curve), is quite narrow and peaks at 480 nm, that is, at the same position as FC*. In addition, its peak amplitude is twice as high as that in FC*, that is, the oscillator strength increases upon relaxation. Such behaviour is not easy to explain, because excess energy is lost upon transition (relaxation) from the FC* region to the RS state. This relaxation should result in a red shift of the fluorescence band, which cannot be observed at all. In addition, it is hard to explain how an increase in oscillator strength could be related to this transition. The CTC state shows the expected red shift of the emission spectrum. However, it also has increased oscillator strength compared to the FC* state. All these spectral properties are not readily explained for a molecule undergoing the structural relaxations on the way to the photoproduct. On modifying the ratio of branching into RS and CTC intermediates, spectra with even more unrealistic properties are obtained. Reducing the efficiency of formation of the RS state increases its oscillator strength even more. For a reduced efficiency of CTC state formation, the related CTC emission spectrum is considerably increased in oscillator strength.

A second reaction model with equal branching into the RS and CTC states is shown in Figure 4c. As a modification to the model described above (Figure 4b) we added a reaction path from the RS state to CTC and thus modelled the reaction schemes proposed in the literature.[33,34] The spectra in Figure 4c were calculated by using a 1/1 branching ratio from the RS state. The spectrum obtained for the FC* state is identical to that calculated for the models used in Figures 4a and b. Comparing the spectra of the FC* and CTC states leads to reasonable interpretations: There is no pronounced increase in oscillator strength and the whole emission spectrum is red-shifted. However, the spectrum of the RS state again shows a strong increase in oscillator strength and no red shift. Both features can not easily be explained. The use of different branching ratios for the transitions FC*→RS/CTC (Figures 4a, 4b) and RS→CTC/S_0 (Figure 4c) does not improve the spectral features if the state RS is formed with high efficiency and if internal conversion from the RS state plays a minor role. Thus, under these conditions the most likely reaction model is sequential.

4. Conclusions: The Reaction Model

Different experimental techniques have been used to investigate the photochemical *Z*→*E* reaction of the HTI ω-amino acid switch. Together with the modelling procedure for the spectral properties of the intermediates, the results can be summarized in the sequential reaction model shown in Figure 5. Optical excitation leads to population of a sequence of three states: the FC* state, the relaxed state RS, and the CTC state with charge-transfer character. The main reaction route is marked by bold black arrows.

The excited-state reaction dynamics after optical excitation of the *Z*-isomer with a blue photon (387 or 402 nm) start in the Franck–Condon region (FC*). Formation of the FC* state changes the dipole moment of the *Z*-structure: single- and double-bond characters are inverted. Rapid relaxation and solvation processes lead to the transition to the relaxed state RS. These processes cause a weak dynamic Stokes shift of the fluorescence emission on a timescale of 200 fs. The molecule in

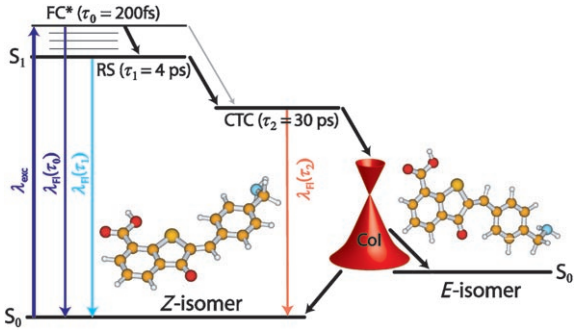

Figure 5. State model for HTI photoisomerization in the *Z*→*E* direction showing all involved states with their corresponding lifetimes. Radiative processes are marked by colored arrows $\lambda_{FI}(\tau)$. The displayed *Z*/*E* structures were optimized with Gaussian 98.

the RS state still has some excess energy which can initiate further conformational changes. In the next process, which occurs on the timescale of 4 ps, a pronounced change in the emission and absorption properties of the molecule can be found. The decay of the blue part of the fluorescence emission and the changes in the transient absorption spectrum support the interpretation that the molecule has undergone a certain charge-transfer reaction during the RS→CTC transition. The final reaction, a transition from the CTC state to the ground state of either the original *Z*-form or the isomeric *E*-form is the key point of the reaction. Starting from the CTC state the molecule must change its shape to reach a critical geometry in which the transition to the ground-state photoproduct can occur. In the transition region the central double bond is rotated by a large angle of about 90°.[2,3,12,15–19] In this geometry the molecule crosses to the ground state presumably through a conical intersection. Here, the reaction branches into starting material *Z* or product *E* with a certain ratio.[18,19] The time constant of about 30 ps observed for this reaction indicates that the transition region can only be reached from the CTC state via a potential barrier. The existence of such a barrier could be shown with temperature-dependent TA measurements on related HTI compounds and will be discussed in a forthcoming paper. A remaining question concerns the reaction coordinate and the exact structure of the intermediates. Rotation around the central double bond, single-bond twists of the hemistilbene moiety, solvation processes, and deformation of the former aromatic rings must be considered. As the CTC state has appreciable charge-transfer character, the double bond is already twisted to a certain extent. The literature describes the transition region in the case of stilbene as a P* state with a 90° twist of the bond angle.[16,17] This state shows extremely short lifetimes[18,19] due to very efficient internal conversion or easy access to a conical intersection. Now the question arises whether the 90° double-bond twist is already reached in the CTC state. In this case the CTC state would be identical to P*. Two arguments seem to exclude this possibility: 1) The potential-energy surfaces of ground and excited states in this 90° position should be very close. This situation suggests a transition to the ground state which is much faster than the observed 30 ps. 2) The proximity between the potential-energy surfaces should prohibit fluorescence emission in the visible spectral range, which is, however, observed for the CTC state. Apparently, it is only after the final 30 ps reaction that the molecule overcomes the barrier which gives access to a critical structure (P*/CoI) with a twist of about 90° and efficient access to the *Z*/*E* ground state. The sequential nature of the reaction and the observed ground-state recovery on the 30 ps timescale suggest that chemical modifications of the molecule will allow the isomerization reaction to be optimized.

Acknowledgements

T.C. and B.H. gratefully acknowledge scholarships donated by the Fonds der Chemischen Industrie. The authors thank P. Gilch and W. Fuß for helpful discussions and many critical comments. We thank A.-K. Siebenborn for careful reading of the manuscript. The work was supported by the Deutsche Forschungsgemeinschaft through the DFC-Cluster of Excellence Munich-Centre for Advanced Photonics and SFB533, B9.

Keywords: isomerization · photochemistry · photochromism · time-resolved spectroscopy · ultrafast spectroscopy

[1] C. Dugave, L. Demange, *Chem. Rev.* **2003**, *103*, 2475 – 2532.
[2] D. H. Waldeck, *Chem. Rev.* **1991**, *91*, 415 – 436.
[3] H. Meier, *Angew. Chem.* **1992**, *104*, 1425 – 1446; *Angew. Chem. Int. Ed. Engl.* **1992**, *31*, 1399 – 1450.
[4] M. Seibold, H. Port, *Chem. Phys. Lett.* **1996**, *252*, 135 – 140.
[5] S. Sporlein, H. Carstens, H. Satzger, C. Renner, R. Behrendt, L. Moroder, P. Tavan, W. Zinth, J. Wachtveitl, *Proc. Natl. Acad. Sci. USA* **2002**, *99*, 7998 – 8002.
[6] J. Wachtveitl, S. Spoerlein, H. Satzger, B. Fonrobert, C. Renner, R. Behrendt, D. Oesterhelt, L. Moroder, W. Zinth, *Biophys. J.* **2004**, *86*, 2350 – 2362.
[7] T. Cordes, D. Weinrich, S. Kempa, K. Riesselmann, S. Herre, C. Hoppmann, K. Rück-Braun, W. Zinth, *Chem. Phys. Lett.* **2006**, *428*, 167 – 173.
[8] T. Hugel, N. B. Holland, A. Cattani, L. Moroder, M. Seitz, H. E. Gaub, *Science* **2002**, *296*, 1103 – 1106.
[9] S. L. Dong, M. Loeweneck, T. E. Schrader, W. J. Schreier, W. Zinth, L. Moroder, C. Renner, *Chem. Eur. J.* **2006**, *12*, 1114 – 1120.
[10] P. Ettmayer, D. France, J. Gounarides, M. Jarosinski, M. S. Martin, J. M. Rondeau, M. Sabio, S. Topiol, B. Weidmann, M. Zurini, K. W. Bair, *J. Med. Chem.* **1999**, *42*, 971 – 980.
[11] C. Garcia-Echeverria, P. Furet, B. Gay, H. Fretz, J. Rahuel, J. Schoepfer, G. Caravatti, *J. Med. Chem.* **1998**, *41*, 1741 – 1744.
[12] M. Klessinger, J. Michl, *Exited States and Photochemistry of Organic Molecules*, VCH, Weinheim, **1995**, p. 369.
[13] G. Orlandi, W. Siebrand, *Chem. Phys. Lett.* **1975**, *30*, 352 – 354.
[14] G. Hohlneicher, B. Dick, *J. Photochem.* **1984**, *27*, 215 – 231.
[15] J. Saltiel, J. L. Charlton, *Rearrangements in Ground and Excited States*, Academic Press, New York, **1980**, p. 25.
[16] J. Saltiel, *J. Am. Chem. Soc.* **1967**, *89*, 1036 – 1037.
[17] J. Saltiel, *J. Am. Chem. Soc.* **1968**, *90*, 6394 – 6400.
[18] W. Fuß, C. Kosmidis, W. E. Schmid, S. A. Trushin, *Angew. Chem.* **2004**, *116*, 4273 – 4277; *Angew. Chem. Int. Ed.* **2004**, *43*, 4178 – 4182.
[19] W. Fuß, C. Kosmidis, W. E. Schmid, S. A. Trushin, *Chem. Phys. Lett.* **2004**, *385*, 423 – 430.
[20] J. A. Syage, W. R. Lambert, P. M. Felker, A. H. Zewail, R. M. Hochstrasser, *Chem. Phys. Lett.* **1982**, *88*, 266 – 270.
[21] S. Herre, W. Steinle, K. Rück-Braun, *Synthesis* **2005**, 3297 – 3300.
[22] W. Steinle, K. Rück-Braun, *Org. Lett.* **2003**, *5*, 141 – 144.
[23] M. Seel, E. Wildermuth, W. Zinth, *Meas. Sci. Technol.* **1997**, *8*, 449 – 452.
[24] R. Huber, H. Satzger, W. Zinth, J. Wachtveitl, *Opt. Commun.* **2001**, *194*, 443 – 448.
[25] T. Schrader, A. Sieg, F. Koller, W. Schreier, Q. An, W. Zinth, P. Gilch, *Chem. Phys. Lett.* **2004**, *392*, 358 – 364.
[26] B. Schmidt, C. Sobotta, S. Malkmus, S. Laimgruber, M. Braun, W. Zinth, P. Gilch, *J. Phys. Chem. A* **2004**, *108*, 4399 – 4404.
[27] B. Schmidt, S. Laimgruber, W. Zinth, P. Gilch, *Appl. Phys. B* **2003**, *76*, 809 – 814.
[28] Gaussian 98 (Revision A.7), M. J. Frisch, G. W. Trucks, H. B. Schlegel, G. E. Scuseria, M. A. Robb, J. R. Cheeseman, V. G. Zakrzewski, J. A. Montgomery, R. E. Stratmann, J. C. Burant, S. Dapprich, J. M. Millam, A. D. Daniels, K. N. Kudin, M. C. Strain, O. Farkas, J. Tomasi, V. Barone, M. Cossi, R. Cammi, B. Mennucci, C. Pomelli, C. Adamo, S. Clifford, J. Ochterski, G. A. Petersson, P. Y. Ayala, Q. Cui, K. Morokuma, D. K. Malick, A. D. Rabuck, K. Raghavachari, J. B. Foresman, J. Cioslowski, J. V. Ortiz, B. B. Stefanov, G. Liu, A. Liashenko, P. Piskorz, I. Komaromi, R. Gomperts, R. L. Martin, D. J. Fox, T. Keith, M. A. Al-Laham, C. Y. Peng, A. Nanayakkara, C. Gonzalez, M. Challacombe, P. M. W. Gill, B. G. Johnson, W. Chen, M. W. Wong, J. L. Andres, M. Head-Gordon, E. S. Replogle, J. A. Pople, Gaussian, Inc., Pittsburgh, PA, **1998**.

[29] W. Holzapfel, U. Finkele, W. Kaiser, D. Oesterhelt, H. Scheer, H. U. Stilz, W. Zinth, *Proc. Natl. Acad. Sci. USA* **1990**, *87*, 5168 – 5172.
[30] S. Schmidt, T. Arlt, P. Hamm, H. Huber, T. Naegele, J. Wachtveitl, W. Zinth, M. Meyer, H. Scheer, *Spec. Chem. Acta A* **1995**, *51*, 1565 – 1578.
[31] P. Hamm, *Chem. Phys.* **1995**, *200*, 415 – 429.
[32] W. Baumann, H. Bischof, J. C. Frohling, C. Brittinger, W. Rettig, K. Rotkiewicz, *J. Photochem. Photobiol. A* **1992**, *64*, 49 – 72.
[33] E. Abraham, J. Oberle, G. Jonusauskas, R. Lapouyade, C. Rulliere, *J. Photochem. Photobiol. A* **1997**, *105*, 101 – 107.
[34] A. K. Singh, P. K. Hota, *J. Phys. Org. Chem.* **2006**, *19*, 43 – 52.

Received: March 30, 2007
Published online on July 5, 2007

